Virus Research 251 (2018) 22–33

Contents lists available at ScienceDirect

Virus Research

journal homepage: www.elsevier.com/locate/virusres

In vitro and *in silico* studies reveal capsid-mutant Porcine circovirus 2b with novel cytopathogenic and structural characteristics

Taís Fukuta Cruz[a,b,*], Angelo José Magro[b,c,*], Alessandra M.M.G. de Castro[d,1], Francisco J. Pedraza-Ordoñez[e], Miriam Harumi Tsunemi[f], David Perahia[g,**], João Pessoa Araujo Jr.[a,b,*]

[a] Departamento de Microbiologia e Imunologia, Instituto de Biociências (IB), Universidade Estadual Paulista (Unesp), Botucatu, São Paulo, Brazil
[b] Instituto de Biotecnologia (IBTEC), Universidade Estadual Paulista (Unesp), Botucatu, São Paulo, Brazil
[c] Departamento de Bioprocessos e Biotecnologia, Faculdade de Ciências Agronômicas (FCA), Universidade Estadual Paulista (Unesp), Botucatu, São Paulo, Brazil
[d] Departamento de Medicina Veterinária Preventiva e Saúde Animal, Universidade de São Paulo (USP), São Paulo, São Paulo, Brazil
[e] Departamento de Salud Animal, Universidad de Caldas, Manizales, Caldas, Colombia
[f] Departamento de Bioestatística, Instituto de Biociências (IB), Universidade Estadual Paulista (Unesp), Botucatu, São Paulo, Brazil
[g] Laboratoire de Biologie et de Pharmacologie Appliquée, ENS Cachan/Université Paris-Saclay, Cachan, France

ARTICLE INFO

Keywords:
Porcine circovirus
PCV2b mutants
Amino acid mutations
Cap protein
Viral replication
Molecular modeling

ABSTRACT

Porcine circovirus 2 (PCV2) is an icosahedral, non-enveloped, and single-stranded circular DNA virus that belongs to the family *Circoviridae*, genus *Circovirus*, and is responsible for a complex of different diseases defined as porcine circovirus diseases (PCVDs). These diseases – including postweaning multisystemic wasting syndrome (PMWS), enteric disease, respiratory disease, porcine dermatitis and nephropathy syndrome (PDNS), and reproductive failure – are responsible for large economic losses in the pig industry. After serial passages in swine testicle (ST) cells of a wild-type virus isolated from an animal with PMWS, we identified three PCV2b viruses with capsid protein (known as Cap protein) cumulative mutations, including two novel mutants. The mutant viruses were introduced into new ST cell cultures for reisolation and showed, in comparison to the wild-type PCV2b, remarkable viral replication efficiency ($> 10^{11}$ DNA copies/ml) and cell death *via* necrosis, which were clearly related to the accretion of capsid protein mutations. The analysis of a Cap protein/capsid model showed that the mutated residues were located in solvent-accessible positions on the external PCV2b surface. Additionally, the mutated residues were found in linear epitopes and participated in pockets on the capsid surface, indicating that these residues could also be involved in antibody recognition. Taking into account the likely natural emergence of PCV2b variants, it is possible to consider that the results of this work increase knowledge of *Circovirus* biology and could help to prevent future serious cases of vaccine failure that could lead to heavy losses to the swine industry.

1. Introduction

Porcine circovirus 2 (PCV2) is a small (17 nm in diameter), icosahedral, non-enveloped, and single-stranded circular DNA virus belonging to the family *Circoviridae*, genus *Circovirus*, which is responsible for a complex of different diseases defined as porcine circovirus diseases (PCVDs) (Segalés, 2012). These diseases – including postweaning multisystemic wasting syndrome (PMWS), enteric disease, respiratory disease, porcine dermatitis and nephropathy syndrome (PDNS), and reproductive failure – are responsible for large economic losses in the pig industry at least since 1990s. PCV2 is currently the most important domestic swine pathogen worldwide (Segalés et al., 2013). Until now, genotypes PCV2a, PCV2b, and PCV2c have been identified (Segalés et al., 2008), with PCV2a and PCV2b being the most prevalent worldwide and PCV2c only described in Denmark (Dupont et al., 2008) and in feral pigs from Brazil (Franzo et al., 2015a). Recently, an emerging genotype (PCV2d-mPCV2b) has been proposed (Chae, 2015; Franzo et al., 2015b) based on a virus described initially in China (Guo et al., 2010) and later associated with cases of vaccine failures in other countries (Seo et al., 2014; Xiao et al., 2012).

* Corresponding authors at: Instituto de Biotecnologia (IBTEC), Universidade Estadual Paulista (Unesp), Botucatu, São Paulo, Brazil.
** Corresponding author.
E-mail addresses: tfcruz@yahoo.com.br (T.F. Cruz), magro@fca.unesp.br (A.J. Magro), david.perahia@gmail.com (D. Perahia), jpessoa@ibb.unesp.br (J.P. Araujo).
[1] Present Address: Complexo Educacional Faculdades Metropolitanas Unidas (FMU/HOVET), São Paulo, São Paulo, Brazil.

https://doi.org/10.1016/j.virusres.2018.04.019
Received 13 January 2018; Received in revised form 27 April 2018; Accepted 27 April 2018
Available online 03 May 2018

The PCV2 genome is computationally predicated to encode 11 overlapping open reading frames (ORFs) (Hamel et al., 1998), but only five viral proteins are expressed by its genome. The Rep and Rep' proteins encoded by ORF1 are essential for viral replication (Cheung, 2003). ORF3 encodes a non-structural (NS) protein associated with apoptosis (Liu et al., 2005), while ORF4 encodes NS protein, which plays a role in suppressing caspase activity and regulating CD4+ and CD8 + T lymphocytes during PCV2 infection (He et al., 2013). In turn, ORF2 encodes a molecule composed of 233 or 236 amino acids known as Cap protein, the structural unit of the PCV2 capsid. This multifunctional protein is considered the main antigenic determinant of the virus (Guo et al., 2011; Nawagitgul et al., 2000); indeed, four linear immunorelevant epitopes (Mahé et al., 2000) and five different overlapping conformational epitopes (Lekcharoensuk et al., 2004) have been identified in the PCV2 Cap protein. The immunogenic epitopes previously identified (Mahé et al., 2000) were also mapped on a crystal structure of an N-terminally truncated PCV2 virus-like particle at 2.3-Å resolution (Khayat et al., 2011). Additionally, regions of amino acid heterogeneity in the Cap protein of different PCV2 strains were identified as important molecular segments for dominant immune response (de Boisséson et al., 2004; Grau-Roma et al., 2008; Larochelle et al., 2002; Timmusk et al., 2008; Wen et al., 2005). Hence, selective pressures on these regions could lead to the emergence of PCV2 variants (Larochelle et al., 2002) with conformational changes in neutralizing epitopes (Huang et al., 2011; Liu et al., 2013; Saha et al., 2012a,b) that may be related to vaccine failure.

Moreover, it has been suggested that the virulence properties of PCV2 seem to be related to the Cap protein (Guo et al., 2011). A link between Cap protein variation and PCV2 pathogenicity is strongly suggested because modifications of the viral capsid may alter determinants involved in tissue tropism and, consequently, could play a key role in the PCV2 replication cycle and virus-host interactions (Larochelle et al., 2002). Therefore, mutations in ORF2 PCV2 may also lead to the emergence of variants with increased *in vivo* virulence, as corroborated by some works involving PCV2d-mPCV2 isolated from an aborted pig with PMWS (Guo et al., 2012) or variants that are attenuated after serial passages in PK-15 cell culture (Fenaux et al., 2004). In this last work, the authors enhanced the *in vitro* growth ability of PCV2 after 120 passages and found two amino acid mutations (P110A and R191S) in the Cap protein, suggesting an association between the protein modifications and viral replication. However, structural analysis of these mutations in the Cap protein was not performed and the authors did not report the occurrence of a cytopathogenic effect (CPE) in the infected PK-15 cells.

Therefore, PCV2 mutations can be found in variants circulating in the field induced by cell culture passages or chemical mutagenesis techniques. Based on the above findings and considerations, it is vital to carry out *in vitro* and *in vivo* studies to characterize these mutants and map amino acid mutations, which may dramatically influence the viral structure and its biological functions. Recently, in our laboratory, it was possible to identify three PCV2b mutants, including two novel mutants, after serial passages in swine testicle (ST) cells of a wild-type virus isolated from an animal with PMWS, with evident CPE and increased viral replication. Members of the genus *Circovirus* are in general considered non-cytopathogenic, difficult to isolate in cell culture, and produce low viral titers (Chen et al., 2013; Meerts et al., 2005). However, subpopulations of the PK-15 cell line infected with PCV2 have been described to present enhanced viral replication associated with CPE (Chen et al., 2013), and the fetal porcine retinal cell line (VR1BL) challenged with a large amount of PCV2b showed CPE due to apoptosis (Dvorak et al., 2013); however, the authors did not analyze the appearance of PCV2 mutations. DNA sequencing of the mutant viruses identified in this work revealed amino acid mutations in the Cap protein, indicating the possible association between structural conformational changes and the cell effects observed *in vitro*.

Thus, to study the main characteristics of these new PCV2b viruses, questions related to their cytopathogenic effects, increased viral replication in ST cells, and the expression of caspase-3, caspase-8 and p53 mRNAs were analyzed. In addition, a structural model was built to

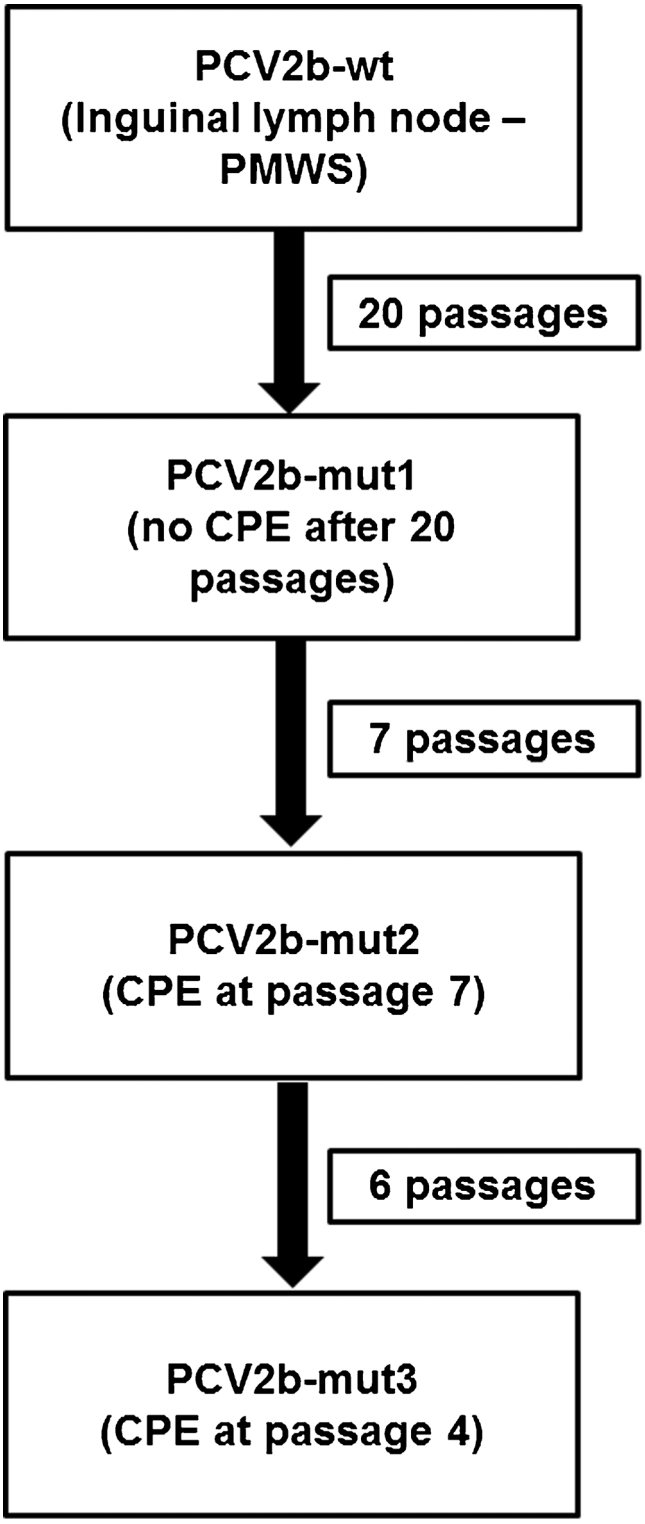

Fig. 1. PCV2b mutants isolated after serial passages in swine testicle (ST) cells. Initially, ST cells were inoculated with wild-type PCV2b (PCV2b-wt) obtained from an inguinal lymph node of a piglet with PMWS. Next to the black arrows is shown the total number of passages for each viral isolation. The parentheses indicate the passage in which the cytopathogenic effect (CPE) was detected in ST cells infected with PCV2 mutants (PCV2b-mut1, PCV2b-mut2, and PCV2b-mut3).

evaluate the position of the mutations in the Cap protein and possible epitope alterations. This structural analysis was performed to gain insights into the immunogenic/antigenic characteristics of PCV2b mutants and to identify relevant structural/function correlations potentially associated with the biological effects observed *in vitro*.

2. Materials and methods

2.1. Cells and viruses

In this study, PCV2b viruses with amino acid mutations in the capsid gene (ORF2) were obtained by intensive serial passages using a swine testicle (ST) PCV1-free cell line provided by Institute for Technological Research (IPT)/University of São Paulo (USP) and treated with 100 mM D-glucosamine (Fig. 1). Initially, the wild-type PCV2b virus (PCV2b-wt) was isolated from an inguinal lymph node sample of a pig from southern Brazil with typical clinical signs of PMWS. For this isolation, the PCV2b infected cells were serially subcultured 20 times and harvested by freeze-thawing three times (Cruz and Araujo Jr, 2014), achieving a high viral load (10^{12} DNA copies/ml ST cell suspensions). The PCV2b virus stock obtained from the previous procedures was designated PCV2b-mut1 (identification of the mutation T200I). The PCV2b-mut1 was then inoculated into a new ST cell culture, and the posterior viral isolation was performed by traditional adsorption as described (Cruz and Araujo Jr, 2014). During this viral isolation, the occurrence of CPE in ST cells infected with PCV2b was observed after the seventh passage ($10^{10.94}$ DNA copies/ml ST cell suspensions). The freeze-thawing procedure was repeated, and the virus stock was assigned as PCV2b-mut2 (identification of mutations T200I and M72I). The PCV2b-mut2 was inoculated into a new ST cell culture, and the virus was passaged until the sixth passage ($10^{11.15}$ DNA copies/ml ST cell suspensions); however, the formation of CPE occurred in the fourth passage ($10^{10.44}$ DNA copies/ml ST cell suspensions). The freeze-thawing procedure was then repeated three times, and this new viral stock was termed PCV2b-mut3 (identification of mutations T200I, M72I, and N77D). The position of the mutations have been numbered according to PCV2b-wt (GenBank KF374705).

2.2. Evaluation of CPE and viral replication in ST cells

To study CPE and viral replication in ST cells, the PCV2b-wt and mutants were reisolated by serially passages. The viral isolation with traditional adsorption was performed as previously described (Cruz and Araujo Jr, 2014), but treatment with 100 mM D-glucosamine was not adopted to assess virus replication in ST cells without induction. Briefly, ST cells with semiconfluent monolayer (25-cm^2 flasks) were inoculated (0.5 ml) with 10% inguinal lymph node suspension PCV2b-wt ($10^{6.47}$ $TCID_{50}$), PCV2b-mut1 ($10^{6.11}$ $TCID_{50}$), PCV2b-mut2 ($10^{6.40}$ $TCID_{50}$), and PCV2b-mut3 ($10^{6.70}$ $TCID_{50}$). The subcultures (1:2) were completed in 48 h at 37 °C with minimum essential medium (MEM) (Gibco, Grand Island, USA) supplemented with 1 mmol/l sodium pyruvate, 0.1 mmol/l non-essential amino acids, 2 mmol/l l-glutamine, 17.86 mmol/l sodium bicarbonate, 25 mmol/l HEPES, and 10% fetal bovine serum (FBS) (Gibco, Grand Island, USA). ST cells (control flask) were inoculated with MEM. To evaluate viral replication, aliquots (intracellular viruses) were separated from the infected and control cell suspensions after trypsinization for DNA and RNA extraction. A total of 16 passages was performed, but fewer were performed for some PCV2b mutants due to severe cell death. For microscopic evaluation and cell counting, one flask of each subculture was fixed with methanol and stained with Giemsa (Freshney, 2000), except the flasks of the first passage. Cell counting was performed in ten different randomly selected fields, and a magnification of 400X was used for evaluation. The results are expressed as the mean number of ST cells/field.

2.3. Nucleic acid extraction and reverse transcription

DNA was extracted from 100 µl of the aliquots collected from each passage using the Illustra blood genomic Prep Mini Spin kit (GE Healthcare, Buckinghamshire, UK) according to the manufacturer's instructions. The extracted DNA was eluted with 100 µl of nuclease-free water. RNA was extracted (100 µl, 2×10^5 ST cells) using the Total RNA Purification kit (Norgen Biotek Corporation, Thorold, Canada) and eluted with 50 µl of nuclease-free water following the manufacturer's instructions. To remove contaminating DNA, extracted RNA was treated with DNase I (Sigma, Saint Louis, USA) according to the manufacturer's protocol. Reverse transcription (RT) for synthesis of complementary DNA (cDNA) was performed using the ImProm-II RT kit (Promega, Madison, USA) with random primers (12.5 ng/µl) according to the manufacturer's instructions.

2.4. Quantitative PCR (qPCR) for viral DNA

The PCV2b viral load was determined after each passage. Extracted DNAs were analyzed by qPCR with 0.4 µM of primers for ORF2 (Larochelle et al., 1999) using the Maxima SYBR Green qPCR Master Mix kit (2x) (Fermentas, Vilnius, Lithuania). The reaction conditions were as follows: 95 °C/10 min, 40 cycles at 95 °C/15 s and 60 °C/1 min (7300 Real Time PCR System, Life Technologies, Foster City, USA). The qPCR limit of detection (1.6×10^1 copies/µl) was determined with a standardized plasmid diluted serially in ten-fold increments from 1.6×10^{11} to 1.6 copies/µl, with a coefficient of correlation (R^2) of 0.99 and an assay efficiency of 97.90% calculated by the standard curve. The concentration of viral DNA was determined by absolute quantification and defined as the number of DNA copies per milliliter of ST cell suspension.

2.5. Reverse transcription-quantitative PCR (RT-qPCR) for viral mRNA and caspase-3, caspase-8 and p53 mRNAs

RT-qPCR was performed to quantify the expression of the Cap protein (ORF2), caspase-3, caspase-8 and p53 mRNAs, using as an endogenous control mRNA of swine glyceraldehyde-3-phosphate dehydrogenase (GAPDH). The RT-qPCR was prepared using the Maxima SYBR Green qPCR Master Mix (2X) kit (Fermentas, Vilnius, Lithuania), and the reaction conditions were 95 °C/10 min, 40 cycles at 95 °C/15 s followed by specific annealing-extension temperatures/1 min (7300 Real Time PCR System, Life Technologies, Foster City, USA). The primer concentrations and annealing-extension temperatures of each target gene were as follows: ORF2 (0.4 µM; 60 °C) (Larochelle et al., 1999), caspase-8 (0.3 µM; 61 °C) (Duran et al., 2009), p53 (0.3 µM; 61 °C) (Duran et al., 2009), and GAPDH (0.3 µM; 60 °C) (Cruz and Araujo Jr, 2014). For RT-qPCR of caspase-3, the forward (5′−CCGGA ATGGCATGTCGAT -3′) and reverse (5′- TGAAGGTCTCCCTGAGATTT -3′) primers were used at 0.3 µM with an annealing-extension temperature of 60 °C. The concentrations of mRNAs for each target gene were normalized to the concentrations of GAPDH, and relative quantification by the standard curve method was used (Larionov et al., 2005). All DNase I-treated RNA samples were analyzed by qPCR with 0.4 µM of primers for ORF1 (Ladekjaer-Mikkelsen et al., 2002) to rule out amplification due to DNA contamination.

2.6. Sequencing of PCV2b isolates in ST cells

The PCV2b-wt and mutants (PCV2b-mut1, PCV2b-mut2, and PCV2b-mut3) used as inoculum, PCV2b isolates from the fifth passage ($PCV2b\text{-}wt^{P5}$, $PCV2b\text{-}mut1^{P5}$, and $PCV2b\text{-}mut2^{P5}$), last passage before cell death ($PCV2b\text{-}mut1^{P12}$, $PCV2b\text{-}mut2^{P11}$, and $PCV2b\text{-}mut3^{P4}$), and last passage of wild-type PCV2b ($PCV2b\text{-}wt^{P16}$) were subjected to complete genomes sequencing. Four primer pairs designed to amplify four overlapping fragments of PCV2b were used as previously described

Table 1
Nucleotide mutation at position A645G, amino acid mutations at positions M72I, N77D, and T200I in the ORF2 gene (capsid protein) of PCV2b, DNA viral load detected by quantitative PCR, and occurrence of cytopathogenic effects (CPE) during serial passages in swine testicle (ST) cells.

PCV2b	Passages	Viral load[a]	CPE	Amino acid mutations			Nucleotide mutations
				T200I 1st[b]	M72I 2nd[b]	N77D 3rd[b]	A645G
PCV2b-wt	inoculum	11.22	–	T	M	N	A
PCV2b-wt^{P5}	5	9.32	no	T	M	N	A
PCV2b-wt^{P16}	16	8.01	no	T	M	N	A
PCV2b-mut1	inoculum	10.94	–	**I**	M	N	A
PCV2b-mut1^{P5}	5	10.26	no	**I**	M	N	A
PCV2b-mut1^{P12}	12	10.36	yes	**I**	**I**	N	**G**
PCV2b-mut2	inoculum	11.06	–	**I**	**I**	N	**G**
PCV2b-mut2^{P5}	5	10.06	no	T/**I**	**I**	**D**	A/**G**
PCV2b-mut2^{P11}	11	10.62	yes	T/**I**	**I**	**D**	A/**G**
PCV2b-mut3	inoculum	11.88	–	**I**	**I**	**D**	A/**G**
PCV2b-mut3^{P4}	4	10.69	yes	T/**I**	**I**	**D**	A/**G**

Bold text: nucleotide and amino acid mutations.
[a] ORF2-DNA copies/ml ST suspensions (log_{10}).
[b] Order of occurrence of amino acid mutations during serial passages in ST cells.

(An et al., 2007). The amplified PCR products with expected molecular sizes were excised from 1.0% agarose gels. The DNA from agarose gels was purified using Illustra GFX PCR DNA and Gel Band Purification kits (GE Healthcare, Buckinghamshire, UK). The purified PCR products were sequenced with both sense and antisense primers using the Big Dye Terminator v.3.1 Cycle Sequencing kit (Life Technologies, Foster City, USA) according to the manufacturer's instructions. Automated sequencing was performed on the ABI 3500 Genetic Analyzer instrument (Life Technologies, Foster City, USA). After sequencing, the Basic Local Alignment Search Tool (BLAST) (https://blast.ncbi.nlm.nih.gov/Blast.cgi) was utilized to confirm the compatibility of the DNA sequences to known PCV2 sequences, and a quality analysis was performed using the Phred program (http://asparagin.cenargen.embrapa.br/phph/). Editing and assembling were performed by using the programs BioEdit v.7.0 (Hall, 1999) and Geneious v.8.0 (Kearse et al., 2012). The nucleotide and amino acid sequences of ORF1, ORF2, ORF3, and ORF4 were aligned using ClustalW (Larkin et al., 2007) implemented in MEGA v.5.2 (Tamura et al., 2011) to compare sequences with the PCV2b-wt sequence (GenBank KF374705).

2.7. Analysis of ORF2 from different PCV2 sequences in the database

One thousand seven hundred twenty PCV2 complete genomes, 999 capsid gene (ORF2) sequences of PCV2 and 60 PCV1 complete genomes available in the GenBank database were analyzed for the presence of nucleotide and amino acid mutations described in this work. Multiple alignments were performed at the nucleotide and amino acid level for the ORF2 gene using ClustalW (Larkin et al., 2007) within MEGA v.5.2 (Tamura et al., 2011) and Geneious v.8.0 (Kearse et al., 2012). These alignments were manually edited to remove sequences with low quality, reading frame errors and early stop codons.

2.8. Cap protein molecular modeling

A molecular model of the PCV2b-mut3 Cap protein was built to verify the position of the mutations M72I, N77D, and T200I. This molecular model was based on the 2.3 Å resolution-crystallographic structure of the capsid from a previously determined consensus sequence of PCV2 (PDB code 3R0R) (Khayat et al., 2011). Initially, a portion composed of nine units of the PCV2b-mut3 Cap protein was separated from the capsid to contain one of its capsomers formed by five units of the Cap protein. The amino acid residues of this nonameric structure were analyzed in relation to their protonation states using the PDB2PQR server (Dolinsky et al., 2004, 2007). The program Charmm v.c36a1 (Brooks et al., 2009) was then used to improve the nonameric structural model: conjugate gradient (CG) and Adopted Basis Newton-Raphson (ABNR) methods of energy minimization were applied to the whole structure with the simultaneous application of harmonic restraints. For this process, the progressive decrease of the harmonic restraints (force 250 to zero) was associated with seven cycles of energy minimization using the conjugate gradient method. For the first six cycles, 100 steps were calculated and the tolerance applied to the average gradient was 1.0. During the seventh and last cycle, 10000 steps were calculated and the tolerance applied to the average gradient was 0.01. Identification of surface pockets of the Cap protein monomers was performed with the LIGSITE^{csc} server (https://omictools.com/ligsitecsc-tool) (Huang and Schroeder, 2006) using a grid space = 1 Å and a probe radius = 5 Å. The C^{α} atom RMSD between all nonameric model monomers and the Cap crystallographic structure was calculated using VMD Molecular Graphics Viewer v.1.9.3 (Humphrey et al., 1996).

2.9. Statistical analysis

The data for the quantification of DNA viral load, mRNA levels, and the cell counting results were analyzed by the Mixed Models with the passages as a random effect (repeated measurements in the same individual). In these analyses, a *P*-value less than 0.05 was considered statistically significant.

2.10. Accession number

The complete sequences of the wild-type and PCV2b mutants reported in this study were deposited in the GenBank database under the following accession numbers: PCV2b-mut1 (GenBank MF150182), PCV2b-mut2 (GenBank MF150183), PCV2b-mut3 (GenBank MF150184), PCV2b-wt^{P5} (GenBank MF150185), PCV2b-mut1^{P5} (GenBank MF150186), PCV2b-mut2^{P5} (GenBank MF150187), PCV2b-wt^{P16} (GenBank MF150188), PCV2b-mut1^{P12} (GenBank MF150189), PCV2b-mut2^{P11} (GenBank MF150190), and PCV2b-mut3^{P4} (GenBank MF150191).

3. Results

3.1. Nucleotide and amino acid mutations in the ORF2 gene (Cap protein)

Four nucleotide transitions were found only in the ORF2 gene (Cap protein) (Table 1). The mutations were observed at nucleotide positions 645 (A645G), 599 (C599T), 216 (G216A), and 229 (A229G) in the PCV2 Cap protein gene. For one mutation (A645G), there were no amino acid changes, but three nucleotide mutations (C599T, G216A,

and A229G) resulted in amino acid changes. The first mutation was observed in PCV2b-mut1 at nucleotide position 599 (C599T) after 20 passages and resulted in a change from threonine to isoleucine (T200I). Then, after seven more passages, a new mutant virus was identified (PCV2b-mut2) that maintained the T200I amino acid mutation and showed two new additional mutations at nucleotide positions 645 (A645G), and 216 (G216A). The second amino acid mutation was found at nucleotide position G216A, which resulted in a methionine to isoleucine substitution (M72I). The mutant PCV2b-mut3 was obtained after four more passages: the previous three nucleotide mutations (A645G, C599T, and G216A) were kept in the capsid gene and remained in subsequent passages. However, a new nucleotide mutation at positon 229 resulted in the third amino acid mutation, in which an asparagine was changed to an aspartic acid (N77D).

The nucleotide and amino acid mutations found during the reisolation were as follows: T200I was observed in the fifth passage of PCV2b-mut1 (PCV2b-mut1^{P5}). T200I and M72I were found in the last passage of PCV2b-mut1^{P12}. T200I, M72I, and N77D were found in the passages of PCV2b-mut2^{P5}, PCV2b-mut2^{P11}, and PCV2b-mut3^{P4}. The silent amino acid mutation (A645G) was found in mutant virus isolates (PCV2b-mut2^{P12}, PCV2b-mut2^{P5}, PCV2b-mut2^{P11}, and PCV2b-mut3^{P4}).

3.2. Analysis of the PCV2 sequences from the GenBank database

After analysis of multiple alignments, 1549 PCV2 complete genomes, 839 ORF2 sequences of PCV2 and 55 PCV1 complete genomes were selected. Consequently, the total of 2388 ORF2 sequences of PCV2 were assessed for the presence of mutations identified in this study (M72I, N77D, and T200I), which were found in 338 sequences. Certain data were not available for selected sequences, so in this study only described information is presented. Six isolates (0.25%) collected from 2007 to 2011 in China and South Korea showed the amino acid mutation 72I. The isolates presented the PCV2a and PCV2b genotype, and one PCV2b isolated from China (GenBank AY847748) was related to PMWS. The largest number of isolates (n = 314; 13.15%), collected from 1994 to 2014, showed the 77D mutation. These isolates were from several countries, such as Australia, Brazil, Canada, China, Croatia, Denmark, France, Germany, Hungary, India, Italy, Japan, Mexico, Portugal, Romania, Serbia, Slovakia, South Africa, South Korea, Spain, Switzerland, Taiwan, and the United States. The genotypes identified in these isolates were PCV2a, PCV2b, and PCV2e, as well the recombinant PCV1/2a. Some isolates (n = 34) presented clinical disorders such as congenital tremors (n = 1), mummified fetuses (n = 1), porcine dermatitis and nephropathy syndrome (PDNS, n = 1), PMWS (n = 29), and sow abortion (n = 2). The 200I amino acid mutation was found in 16 (0.67%) PCV2a and PCV2b isolates from China, Canada, Belgium, Romania, Slovakia, and India, from 2007 to 2012. Two PCV2a isolates from Slovakia (GenBank JN133305) and China (GenBank HM038033) were diagnosed with PMWS. Two isolates (0.084%) from Taiwan and the United States (collected in 2012) presented the nucleotide mutation 645 G in the ORF2 gene, but the genotype and health status were not described for these sequences. Thus, until now, isolates with three Cap protein amino acid mutations (72I, 77D, and 200I) have not been described. Only isolates of the PCV2a genotype with two simultaneous mutations in this protein have been found (Table 2). Four Chinese isolates (GenBank HM038033, JF682791, JF682793, and JF682794) presented the mutations 72I and 200I. The isolates from Canada (GenBank GU049340) and Slovakia (GenBank JN133305) showed mutations 77D and 200I, while those isolated from South Korea (GenBank JF317584) showed mutations 72I and 77D. The 645 G nucleotide and 77D amino acid mutations were found in one isolate from the United States (GenBank KM190985). Fifty-three PCV1 isolates had variable amino acids at positions 72 (glutamine, tyrosine, histidine, and glutamic acid), 77 (isoleucine), and 200 (glycine). The 645 G nucleotide mutation was found in all sequences of PCV1.

3.3. Evaluation of CPE in ST cells infected with PCV2b mutants

The occurrence of CPE was confirmed after serially passaging of PCV2b-mut1, PCV2b-mut2, and PCV2b-mut3 in ST cells. The total passages achieved before cell death was as follows: 12 passages (PCV2b-mut1), 11 passages (PCV2b-mut2), and 4 passages (PCV2b-mut3). CPE was more severe in the 9th passage of PCV2b-mut1 and PCV2b-mut2 and the 3rd passage of PCV2b-mut3. The ST cell control and wild-type virus (PCV2b-wt) did not show CPE and were passed until the 16th passage. The cell counting data comparisons of the ST cell control and PCV2b-wt revealed higher numbers in comparison to PCV2b mutants during viral reisolation; the PCV2b-mut3 had the lowest cell numbers (Fig. 2). The evaluation of mean cell counts between the ST cell control and PCV2b-wt showed no statistically significant differences ($P = 1.0$). On the other hand, the lower mean cell counts of PCV2b mutants differed significantly compared with the ST cell control ($P < 0.0001$) and PCV2b-wt ($P < 0.0001$). The comparison between PCV2b mutants also revealed a statistically significant difference between the lower mean cell count of PCV2-mut3 and PCV2b-mut1 ($P < 0.0001$) and PCV2b-mut3 and PCV2b-mut2 ($P = 0.0001$), while the comparison between PCV2b-mut1 and PCV2b-mut2 showed no significant difference ($P = 0.995$). A microscopic evaluation revealed fusiform to rounded cells that became becoming necrotic with an eosinophilic cytoplasm, condensed chromatin, karyorrhexis, and karyolysis (Fig. 3).

3.4. Increased viral replication of PCV2b mutants in ST cells

The viral loads determined for PCV2b-mut1, PCV2b-mut2, and PCV2b-mut3 were higher than that of the original PCV2b-wt (Fig. 2). The mean viral loads of PCV2b-mut1, PCV2b-mut2, and PCV2b-mut3 were significantly different from the mean viral load of PCV2b-wt ($P < 0.0001$). However, there were no significant differences in the mean viral load between PCV2b-mut1 and PCV2b-mut2 ($P = 0.991$), PCV2b-mut1 and PCV2b-mut3 ($P = 0.295$), PCV2b-mut2 and PCV2b-mut3 ($P = 0.164$). All passages of the ST cell control were negative for PCV2 by qPCR. The occurrence of severe CPE coincided with the peak viral load ($> 10^{11}$ DNA copies/ml ST cell suspensions) in PCV2b-mut1, PCV2b-mut2, and PCV2b-mut3. After the occurrence of CPE, the viral load was lower in the subsequent passages due to cell death. Thus, fewer passages were used for PCV2b-mut3 in comparison to PCV2b-wt, PCV2b-mut1, and PCV2b-mut2.

3.5. Relative expression of ORF2, caspase-3, caspase-8, and p53 mRNAs

The expression of ORF2-mRNA for PCV2b mutants was higher in comparison to PCV2b-wt, and the peaks of viral mRNA expression coincided with the occurrence of CPE, as described above for the viral load (Fig. 2). The mean expression of ORF2-mRNA was significantly higher in PCV2b-mut1, PCV2b-mut2, and PCV2b-mut3 in relation to PCV2b-wt ($P < 0.0001$). However, there were no significant differences in the mean expression of ORF2-mRNA between PCV2b-mut1 and PCV2b-mut2 ($P = 0.655$), PCV2b-mut1 and PCV2b-mut3 ($P = 0.973$), PCV2b-mut2 and PCV2b-mut3 ($P = 0.514$). The mRNA levels of caspase-3, caspase-8, and p53 were slightly elevated in PCV2b mutants and PCV2b-wt in comparison to the ST cell control (Fig. 4), but there was no statistically significant difference in the mean expression of mRNA of caspase-8 ($P > 0.3$) and p53 ($P > 0.7$) in the comparisons performed between these groups. For the mean expression of caspase-3 mRNA, there was a statistically significant difference only for the higher expression of mRNA of PCV2b-mut3 in relation to ST cell control ($P = 0.0424$). All DNase I-treated RNA samples were negative for ORF1-DNA by qPCR.

Table 2
Sequences available in the GenBank database showing more than one mutation in the ORF2 gene (capsid protein) of PCV2a.

Accession Number	Amino acid mutations			Nucleotide mutations	Country	Year	Health status	References
	72I	77D	200I	645G				
HM038033	**I**	N	**I**	A	China	2007	PMWS	Guo et al. (2010)
JF682791	**I**	N	**I**	A	China	2010	Unknown	Guo et al. (2011)
JF682793	**I**	N	**I**	A	China	2011	Unknown	Guo et al. (2011)
JF682794	**I**	N	**I**	A	China	2011	Unknown	Guo et al. (2011)
GU049340	M	**D**	**I**	A	Canada	2007	PMWS	Fort et al. (2010)
JN133305	L	**D**	**I**	A	Slovakia	2009	PMWS	Saha et al. (2012a,b)
JF317584	**I**	**D**	T	A	South Korea	2010	Unknown	Nguyen et al. (2012)
KM190985	M	**D**	T	**G**	USA	2012	Unknown	Xiao et al. (2015)

Bold text: nucleotide and amino acid mutations described in this study.
PMWS: postweaning multisystemic wasting syndrome.

3.6. Cap protein molecular model

The energy-minimized nonameric PCV2b-mut3 Cap protein model presented good stereochemistry, as shown by the MolProbity program (Chen et al., 2010): 98.8% of all residues were in allowed regions of the Ramachandran plot. Additionally, the model showed a good MolProbity score (1.31), an evaluation that takes into account structural parameters such as clashes, rotamers, and stereochemistry (Chen et al., 2010). Additionally, an analysis of the whole structure using the server ProSA-web (Wiederstein and Sippl, 2007) indicated a good Z-score (-4.47). This Z-score indicated an adequate overall quality of the quaternary structural model in comparison to experimentally determined protein chains with similar molecular sizes deposited in the Protein Data Bank (PDB) (Wiederstein and Sippl, 2007). C^{α} atom alignment between all nine monomers in the model and to the Cap crystallographic structure also highlighted the high structural similarity of this molecule, with a RMSD = 1.0 Å. The nonameric and monomeric PCV2b-mut3 Cap models are shown, respectively, in Figs. 5 and 6.

4. Discussion

Mutations in the Cap protein may be related to PCV2 pathogenicity due to alterations of the determinants involved in tissue tropism, the PCV2 replication cycle and the host protective response against viral infection (Larochelle et al., 2002; Opriessnig et al., 2006). The identification of new wild-type-derived PCV2b viruses with Cap protein mutations (PCV2b-mut1 – T200I mutation; PCV2b-mut2 – M72I and T200I mutations; and PCV2b-mut3 – M72I, N77D, and T200I mutations) and the *in vitro* and *in silico* studies showing the notable adaptation of these viruses, their evident cytopathogenic effect (CPE) and suggested important viral characteristics of the PCV2b variants are discussed below.

4.1. CPE and viral replication in wild-type and mutants

According to the evaluation of CPE and cell counting after reisolation, the mean number of ST cells/field remained similar (530 ST cells/field) at passage 2 in the ST cell control, PCV2b-wt, and PCV2b-mut1. However, for PCV2b mutants with two (PCV2b-mut2; 372 ST cells/field) and three amino acid mutations (PCV2b-mut3; 138 ST cells/field), there was a decrease in the mean number of ST cells/field due to the occurrence of CPE with severe cell death (Fig. 2), indicating a remarkable influence of these viruses on cell viability. This effect was especially prominent for the virus with three Cap protein mutations, as highlighted by the evident CPE at passage 3. In contrast, PCV2b-mut1 and PCV2b-mut2 viruses caused evident CPE only at passage 9. Moreover, after the detection of CPE, the PCV2b-mut1 supported three more ST cell passages before severe cell death, while PCV2b-mut2 and PCV2b-mut3 permitted only two and one more ST cell passage before severe cell death, respectively (Fig. 2).

In the microscopic evaluation of the CPE found in ST cells infected with PCV2b, the observed changes were cell death by necrosis. However, PCV2 can induce apoptosis by activating caspase-8 and caspase-3 pathways (Liu et al., 2005) *via* the action of non-structural ORF3 protein, which competes with p53 for binding to Pirh2, deregulating p53 homeostasis (Karuppannan et al., 2010; Liu et al., 2007). Thus, the occurrence of apoptosis was analyzed by RT-qPCR for detecting mRNA expression of caspase-3, caspase-8, and p53 from each passage of the ST cell control and ST cells infected with PCV2b-wt and PCV2b mutants. The mRNA of caspase-3, caspase-8, and p53 was expressed at all passages, but there was no statistically significant difference between caspase-8 and p53. On the other hand, a significantly higher mean expression level of caspase-3 mRNA in PCV2b-mut3 was detected in comparison to the ST cell control ($P = 0.0424$). Thus, according to these results PCV2b-mut3 may have induced a rapid and intense ST cell death *via* necrosis and apoptosis. PCV2 infection of VR1BL cells demonstrated that apoptosis may not be the only mechanism involved in PCV2-mediated cell death since a marked increase in cell death and a small number of early apoptotic cells were observed by flow cytometry (Dvorak et al., 2013). Moreover, it has been reported that different cellular antiviral death programs compete with each other (Agol, 2012). In general terms, mechanisms of necrosis and apoptosis may be activated after virus entry into the cell, synthesized viral proteins may produce positive or negative stimuli for these pathways, and the dominance of one of the mechanisms will depend on the balance between proapoptotic and antiapoptotic factors present in infected cell (Agol, 2012). Therefore, PCV2 produces viral proapoptotic (ORF3 protein) (Liu et al., 2005) and antiapoptotic (ORF4 protein) proteins (He et al., 2013), which may influence the development of necrosis or apoptosis. Consequently, the balance between these mechanisms involved in cell death induced by PCV2 must be elucidated, as suggested by our results.

The occurrence of two amino acid mutations in the PCV2a capsid (P110A and R191S) were reported after 120 viral passages, which enhanced virus replication *in vitro* and attenuated the virus *in vivo* without morphological changes in PK-15 cells (Fenaux et al., 2004). The presence of these mutations was analyzed in PCV2b-wt and PCV2b mutant sequences, but these positions were occupied by the amino acid residues proline (position 110) and glycine (position 191). To analyze the possible effects caused by the mutations M72I, N77D, and T200I on PCV2b replication efficiency, qPCR and RT-qPCR assays were performed. For PCV2b-wt, there was a significant decrease in viral load in comparison to the mutant viruses during viral isolation. In isolates with amino acid mutations, these values were higher and peaked ($> 10^{11}$ DNA copies/ml ST cell suspensions), which coincided with the occurrence of evident CPE. After the maximum peak, there was a decrease in the viral load due to extensive cell death. The same profile was observed for the expression of ORF2-mRNA, with significantly higher viral mRNA levels of mutant viruses in comparison to PCV2b-wt (Fig. 2). Therefore, the three amino acid mutations in the viral capsid could be responsible for the higher replication efficiency of the PCV2b mutants

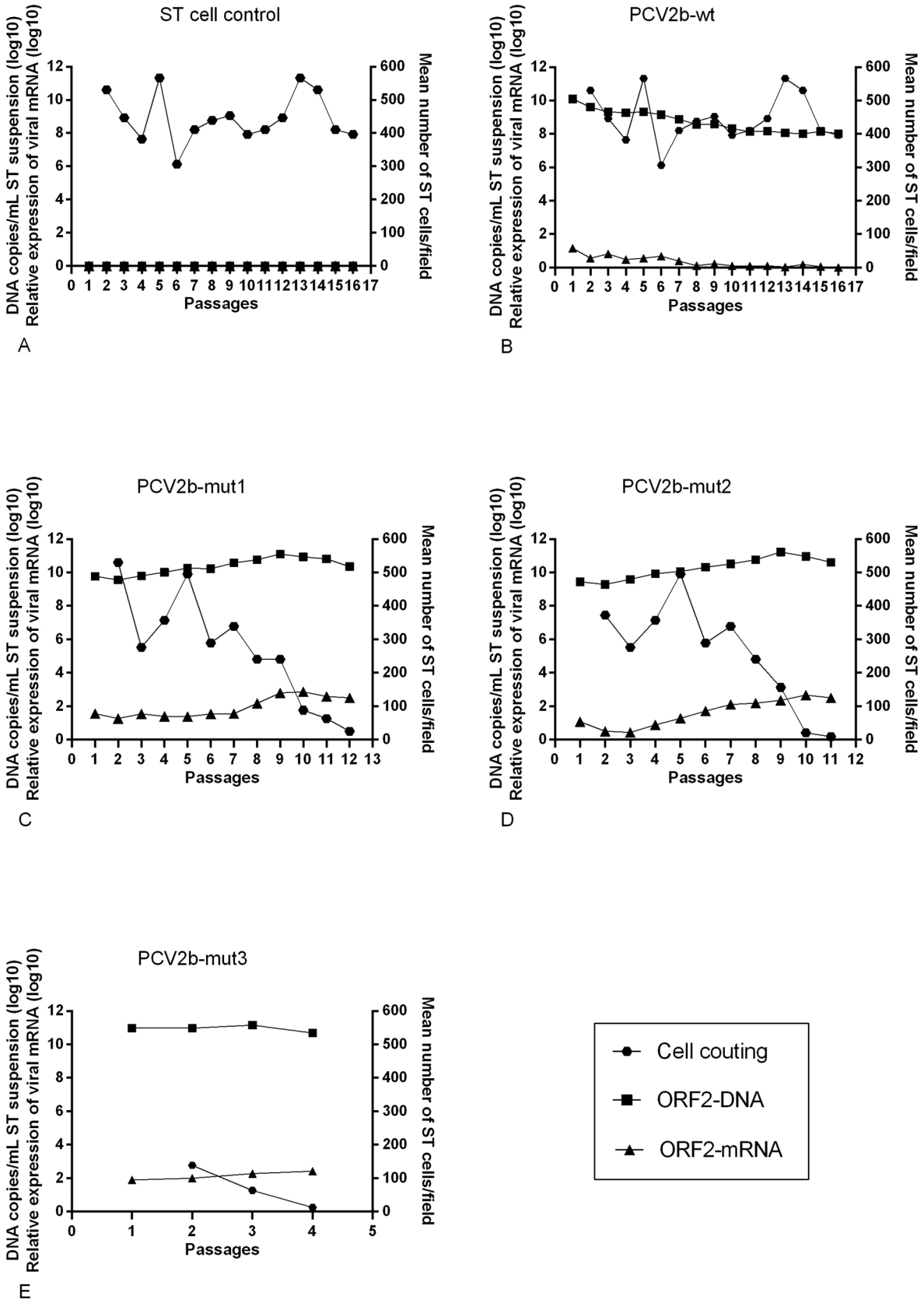

(caption on next page)

Fig. 2. Evaluation of cell survival and viral replication in ST cells infected with PCV2b-wt and mutants. Cell survival was evaluated by cell counting, which revealed a decrease due to the cytopathogenic effect (CPE) with severe cell death, while the replication efficiency was analyzed by determination of the DNA viral load (qPCR) and expression of ORF2-mRNA (RT-qPCR) in swine testicle (ST) cells infected with wild-type PCV2b (PCV2b-wt) and PCV2b mutants (PCV2b-mut1, PCV2b-mut2, and PCV2b-mut3). (A) ST cell control: without virus; no CPE. (B) PCV2b-wt: no CPE. (C) PCV2b-mut1: CPE at passage 9. (D) PCV2b-mut2: CPE at passage 9. (E) PCV2b-mut3: CPE at passage 3. The mean DNA viral load and ORF2-mRNA levels of the PCV2b mutants were significantly higher in relation to PCV2b-wt ($P < 0.0001$). The mean cell counts of the PCV2b mutants were significantly lower than the ST cell control ($P < 0.0001$) and PCV2b-wt ($P < 0.0001$). The mean cell counts of the PCV2b-mut3 were significantly lower in relation PCV2b-mut1 ($P < 0.0001$) and PCV2b-mut2 ($P = 0.0001$). There were no statistically significant differences between the mean cell counts for the ST cell control and PCV2b-wt, the PCV2b-mut1 and PCV2b-mut2, or the mean DNA viral load and ORF2-mRNA expression between PCV2b mutants.

observed in ST cells, leading to severe cell death (CPE) due to cell culture adaptation. However, the *in vivo* response must be investigated since it may be more virulent or attenuated in infected animals. To clarify this issue, assessment of the pathogenicity of PCV2b mutants *in vivo* is currently being carried out by our research group.

4.2. Analysis of the deposited sequences highlights the unique identity of the PCV2 mutants

Taking into account that the accretion of the identified Cap protein mutations is associated with a higher viral replication efficiency and cell death, the combination of the amino acid residues was investigated in 72I, 77D, and 200I in other PCV2 isolates. The presence of two concomitant amino acid mutations was identified in seven PCV2a sequences. Amino acid mutations 72I and 77D were observed in an isolate termed A5293 (GenBank JF317584) from a > 300-day-old piglet with unknown clinical signs (Nguyen et al., 2012) and any information regarding the occurrence of CPE and increased viral replication. Four isolates from China (GenBank HM038033, JF682791, JF682793, and JF682794) had the amino acid mutations 72I and 200I. In this case, a strain identified as CL (GenBank HM038033) was isolated from the lung of a 9-week-old piglet with PMWS and respiratory signs (Guo et al., 2010). The same research group performed a recombination study *in vitro* by PK-15 cell co-infection and obtained new strains from CL (strains PCV2a/CL1, PCV2b/JF11, and PCV2b/YJ) (Guo et al., 2011). In this study (Guo et al., 2011), the authors also reported that two new PCV2b recombinant mutants, (PCV2b(JF11)/2a(CL1) (GenBank JF682793) and PCV2b(YJ)/2a(CL1) (GenBank JF682794), obtained from the posterior recombination of PCV2a/CL1, PCV2b/JF11, and the PCV2b/YJ strains presented an enhanced *in vitro* replication efficiency and antigenicity alterations in comparison to their parental strains. However, these two new PCV2 recombinant mutants did not contain any amino acid or nucleotide mutations in relation to their parental strains, and the occurrence of CPE was not reported. The 77D and 200I mutant combination were observed in two strains deposited in GenBank: the Slovak (GenBank JN133305) (Saha et al., 2012a,b) and Imp.1010-Stoon strains (GenBank GU049340) (Fort et al., 2010). Both strains were obtained from PMWS-affected piglets, and the occurrence of CPE after growth in PK-15 cells was not described. The Imp.1010-Stoon strain (GenBank GU049340) was obtained from the original Imp.1010-Stoon strain (GenBank AF055392) (Meehan et al., 1998), which is referenced in several studies with PCV2 since its isolation (Ellis et al., 1998) and molecular characterization (Meehan et al., 1998). Interestingly, the 77D mutation was present in the original strain (Imp.1010-Stoon), but the 200I mutation was obtained after serial passaging (Fort et al., 2010), as observed in our results. Taken together, these data suggest that the combination of two mutations (72I/77D, 72I/200I, and 77D/200I) present a low frequency but are associated with serial passages in PK-15 cells and/or the occurrence of PMWS. Remarkably, the simultaneous presence of the Cap protein 72I, 77D, and 200I mutations or a double combination of these mutations have not been described for the PCV2b virus to date. Thus, it is clear that the isolates identified herein could present very distinct pathogenic properties in comparison to other wild-type and mutant PCV2a/PCV2b viruses that have been previously studied. Indeed, this hypothesis is strengthened by the findings related to the higher viral replication and evident CPE observed i*n vitro* for the PCV2b mutants.

4.3. Cap protein structural analysis suggests relevant viral characteristics

To evaluate the position of the M72I, N77D, and T200I mutations on the surface of the Cap protein, a structural model containing nine monomers of this molecule was built based on the 2.3 Å resolution crystallographic structure of the capsid from a previously determined consensus sequence of PCV2 (PDB code 3R0R) (Khayat et al., 2011). The nonameric model presents three central monomers of the Cap protein and six additional chains to provide interfacial contacts for the central units (Fig. 5A). This model construction was performed to avoid improper tertiary structure displacement of the central three monomers during the energy minimization process used to improve the whole nonameric structure. The structural analysis of the nonameric model demonstrated that this modeling strategy might be considered

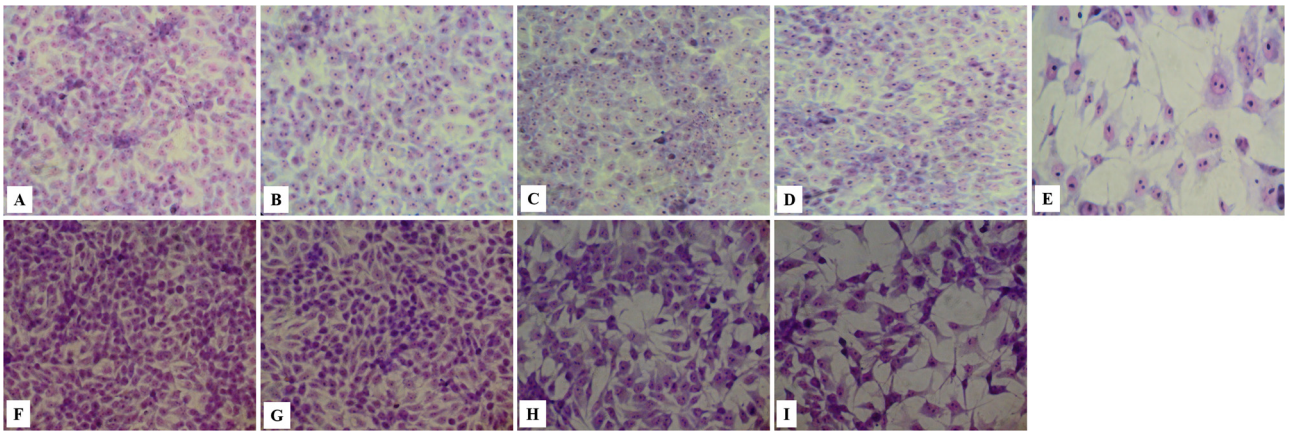

Fig. 3. Cytopathogenic effect (CPE) in swine testicle (ST) cells infected with PCV2b mutants (Giemsa staining). Third passage (A, B, C, D, and E) and ninth passage (F, G, H, and I) cells presented the following results: (A) ST cell control: no CPE. (B) PCV2b-wt^{P3}: no CPE. (C) PCV2b-mut1^{P3}: no CPE. (D) PCV2b-mut2^{P3}: no CPE. (E) PCV2b-mut3^{P3}: CEP. (F) ST cell control: no CPE. (G) PCV2b-wt^{P9}: no CPE. (H) PCV2b-mut1^{P9}: CPE. (I) PCV2b-mut2^{P9}: CPE. Magnification of 400×.

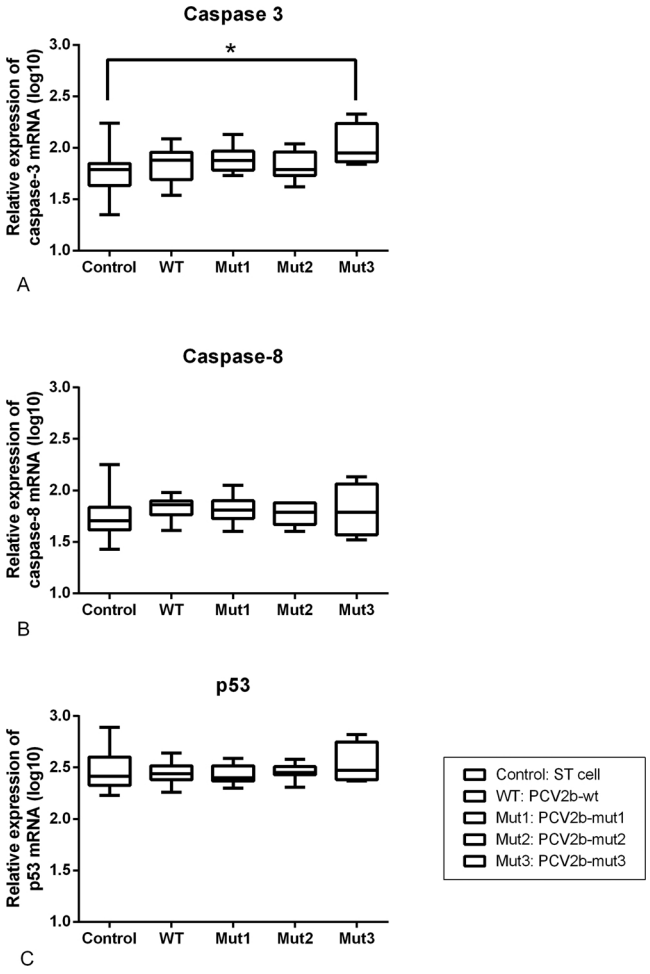

Fig. 4. Levels of caspase-3, caspase-8, and p53 mRNA expression. Swine testicle (ST) cells were infected with wild-type PCV2b (PCV2b-wt) and PCV2b mutants (PCV2b-mut1, PCV2b-mut2, and PCV2b-mut3). The levels of caspase-3, caspase-8, and p53 mRNA expression were determined by RT-qPCR. (A) mRNA expression of caspase-3. (B) mRNA expression of caspase-8. (C) mRNA expression of p53. A significantly higher mean expression level of caspase-3 mRNA in PCV2b-mut3 was found in comparison to the ST cell control by Mixed Models with the passages as a random effect (repeated measurements in the same individual) (*$P < 0.05$).

adequate: 98.8% of all residues were allocated in allowed regions of the Ramachandran plot (Chen et al., 2010), and the MolProbity score (Chen et al., 2010) and Z-score (Wiederstein and Sippl, 2007) (respectively, 1.31 and −4.47) confirmed the overall good stereochemistry of the model. Moreover, a C^{α} atom alignment between all nine monomers of the model and to the Cap crystallographic structure also demonstrated the very similar structures of these molecules (RMSD = 1.0 Å).

As shown in Fig. 5B, the mutated residues 72I, 77D, and 200I were localized in solvent-accessible positions on the external surface of the virus. This finding raises interesting questions about the role of these mutated residues in structural/functional properties of the Cap protein as, for example, cell recognition. As previous described (Misinzo et al., 2006), virus attachment to host cells is a triggering event for infection and can be inherently associated with tissue tropism and pathogenesis. These same authors investigated the role of glycosaminoglycans (GAGs) as molecular receptors for PCV2 based on two points: i) these molecules are important cell receptors for many other viruses (Bernfield et al., 1999; Liu and Thorp, 2002; Rostand and Esko, 1997; Vanderplasschen et al., 1993), and ii) several different cellular types are implicated in PCV2 infection, indicating thus these viruses could identify an ubiquitous cell receptor. Their results indicated that pre-incubation of PCV2 with heparin, heparan sulfate and chondroitin sulfate B was able to reduce infection in porcine monocytic 3D4/31 cells, possibly due to competition with similar receptors present on the cellular surfaces. As demonstrated by the authors, these findings emphasize the importance of specific molecules for PCV2 attachment and posterior infection, given that other GAGS did not avoid viral invasion in 3D4/31 cells. The possible structural/functional effects of the M72I, N77D, and T200I mutations is especially strengthened by the physical-chemical properties of the mutated residues, which present different characteristics in comparison to the new ones added to the Cap protein sequence. As described above, these mutations were cumulative and identified in the following sequence: PCV2b-mut1 presented the T200I mutation, in which a non-charged and polar residue (threonine) was substituted for an aliphatic and hydrophobic one (isoleucine); PCV2b-mut2 showed the mutations T200I and M72I, with the latter characterized by the substitution of a hydrophobic residue with a longer aliphatic side chain and a weakly nucleophilic thioether group (methionine) for another hydrophobic one (isoleucine). The PCV2b-mut3 presented the previous two mutations (M72I and T200I) plus N77D, which is also very remarkable since a non-charged and polar residue (asparagine) was replaced by a negatively charged one (aspartate). In addition, further detailed analysis of the surface of the model revealed that the mutated residues of the whole model were mostly localized in rim regions and/or inside Cap protein cavities (pockets). As previously described, pockets are in general concave-shaped sites where ligands may firmly bind to proteins (Gao and Skolnick, 2012). Remarkably, at the entrance and part of the interior region of a given external Cap protein pocket (herein denominated pocket 1), the residues methionine and threonine at positions 72 and 200 are substituted for two isoleucine residues, making the environment of this pocket predominantly hydrophobic, while the entrance of another external Cap protein pocket (herein denominated pocket 2) becomes negatively charged due to a Asn → Asp mutation (Fig. 6). Additionally, but equally important, the mutated residues also play roles in the linear epitopes identified in antigenic studies of PCV2 with pathogen-free swine (Mahé et al., 2000). Indeed, the M72 and N77 residues (which were mutated in PCV2b-mut2 and PCV2b-mut3) are putative residues found on the external capsid surface that are responsible for discriminating monoclonal antibody binding to PCV1 and PCV2 (Khayat et al., 2011). However, as observed in our model for mutated residue I200, a previous detailed inspection of the Cap protein crystallographic model (Khayat et al., 2011) revealed that the side chain of residue T200 also helped to complete the concave surface of pocket 1, suggesting that this residue could also be involved in antibody recognition. Therefore, there is a clear possibility that the mutant viruses PCV2b-mut1, PCV2b-mut2 and PCV2b-mut3 can provoke cases of vaccine failure if they emerge in nature and reach swine populations.

Finally, taking into account the increased cytopathogenic properties of the PCV2b mutants *in vitro* and their possible immunological/antigenic characteristics, it is evident that a deeper understanding of the biology and structure of these viruses will be valuable to avoid future problems in the swine industry. A feasible solution to prevent upcoming risks to commercial swine populations could be, for example, to produce new vaccines containing artificial capsids with the Cap protein mutations described herein and other identified in future studies.

5. Conclusions

In vitro studies showed that the PCV2b mutants, in comparison to the wild-type virus (PCV2b-wt), presented a higher viral replication efficiency and marked cell death *via* necrosis, which were clearly associated with the accretion of Cap protein amino acid mutations. The amino acid mutations M72I, N77D, and T200I found in the PCV2b mutants were found in two (59–80 and 180–191) of the three Cap protein major variable regions (59–80, 121–136, and 180–191) previously identified (Larochelle et al., 2002) and subsequently confirmed

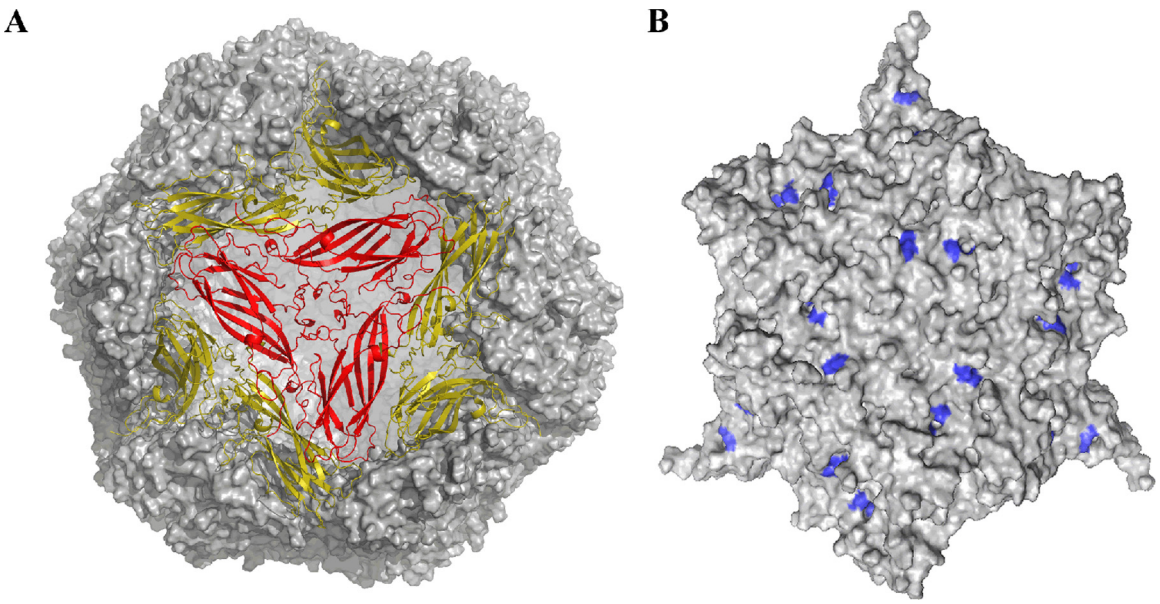

Fig. 5. M72I, N77D, and T200I mutations on the surface of the PCV2b Cap protein. (A) The nonameric model (depicted in cartoon representation) presents at the center three Cap protein monomers (in red) and more six Cap protein monomers (in olive) added to provide interfacial contacts to the central units during the energy minimization cycles used to improve the whole nonameric model. (B) The blue spots indicate the atoms of the mutated residues M72I, N77D, and T200I exposed on the nonameric model surface. Illustration generated with the program PyMOL (DeLano, 2002) (For interpretation of the references to colour in this figure legend, the reader is referred to the web version of this article).

by other authors (de Boisséson et al., 2004; Grau-Roma et al., 2008; Timmusk et al., 2008; Wen et al., 2005). The possible involvement of these highly variable regions in the emergence of PCV2 variants has been reported, mainly owing to two of these regions (59–80 and 121–136) (Larochelle et al., 2002). Hence, the detection of these mutations in the final passages (as shown in Table 1) during viral isolation may be due to the presence of quasispecies in the original viral inoculum (inguinal lymph node suspension) and/or as result of serial passages in cell culture. Although there is no report of quasispecies detection *in vivo* and *in vitro* (Segalés et al., 2013), PCV2 has a high genetic diversity that seems to be generated by the combination of mutations and genetic recombination (Ssemadaali et al., 2015). In fact, PCV2 presents one of the highest rates of nucleotide substitution (approximately 1.2×10^{-3} substitutions/site/year) for a single-stranded DNA virus, very possibly resulting in the rapid emergence of mutants (Firth et al., 2009) and albeit the reason why the high mutation rate of these viruses is still elusive (Firth et al., 2009; Duffy et al., 2008). Furthermore, the spontaneous deamination and higher frequency of C to T transitions are more common in single-stranded DNA viruses due to lack of double helix protection (Lindahl and Nyberg, 1974; Ritchie et al., 2003). Therefore, based on our findings, it is not possible to draw conclusions regarding the nature of the process, leading to the emergence of the identified mutants *in vitro*. However, it is possible that these PCV2b mutants can arise under natural conditions, as demonstrated by the mutations found in database sequences, and provoke severe pathogenic effects *in vivo* as observed *in vitro*. Moreover, analysis

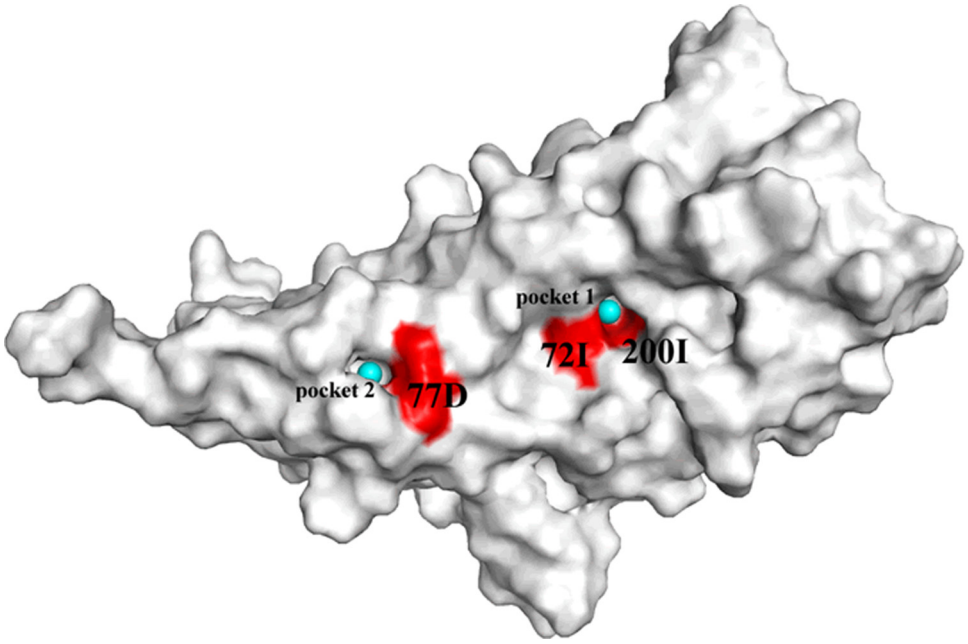

Fig. 6. Solvent-exposed surface (in red) of the mutated amino acid residues found in the Cap protein. The mutations around pockets 1 and 2 (identified with cyan probes) change the physical-chemical properties around their surroundings: methionine and threonine at positions 72 and 200 are substituted for two isoleucine residues, making the environment of the first pocket predominantly hydrophobic, while the Asn → Asp mutation becomes the entrance of the second negatively charged pocket. Illustration generated with the program PyMOL (DeLano, 2002) (For interpretation of the references to colour in this figure legend, the reader is referred to the web version of this article).

of the Cap protein/capsid model showed that the mutated residues 72I, 77D and 200I are localized in solvent-accessible positions on the external PCV2b surface. This structural feature brings attention to a possible role of these mutated residues in structural/functional properties of the Cap protein related to the peculiar pathogenic effect observed *in vitro*. Additionally, the mutated residues are found in linear epitopes and participate in pockets on the capsid surface, indicating thus these residues could also be involved in antibody recognition. Also, our analyses suggest the PCV2b-mut3 can induce cellular death both by necrosis and apoptosis due to the significant caspase-3 expression, indicating thus another explanation to the remarkable pathogenic activity of this virus. Based on our findings and the possibility of natural emergence of the identified PCV2b mutant virus we consider that another *in vitro* and *in vivo* studies should be carried out to avoid cases of vaccine failure and serious losses to the swine industry in the future.

Funding

This work was supported by the São Paulo Research Foundation (FAPESP) [grant numbers 2006/57976-6, 2006/59002-9, and 2013/14530-1]; and the National Council for Scientific and Technological Development (CNPq) [grant numbers 471070/2007-6, 500905/2007-0, and 12748/2008-6].

References

Agol, V.I., 2012. Cytopathic effects: virus-modulated manifestations of innate immunity? Trends Microbiol. 20 (12), 570–576. http://dx.doi.org/10.1016/j.tim.2012.09.003. PMID: 23072900.

An, D.J., Roh, I.S., Song, D.S., Park, C.K., Park, B.K., 2007. Phylogenetic characterization of porcine circovirus type 2 in PMWS and PDNS Korean pigs between 1999 and 2006. Virus Res. 129 (2), 115–122. http://dx.doi.org/10.1016/j.virusres.2007.06.024. PMID: 17706315.

Bernfield, M., Götte, M., Park, P.W., Reizes, O., Fitzgerald, M.L., Lincecum, J., et al., 1999. Functions of cell surface heparan sulfate proteoglycans. Annu. Rev. Biochem. 68, 729–777. http://dx.doi.org/10.1146/annurev.biochem.68.1.729. PMID: 10872465.

Brooks, B.R., Brooks 3rd, C.L., Mackerell Jr, A.D., Nilsson, L., Petrella, R.J., Roux, B., et al., 2009. CHARMM: the biomolecular simulation program. J. Comput. Chem. 30 (10), 1545–1614. http://dx.doi.org/10.1002/jcc.21287. PMID: 19444816.

Chae, C., 2015. An emerging porcine circovirus type 2b mutant (mPCV2b) originally known as PCV2d. Vet. J. 203 (1), 6–9. http://dx.doi.org/10.1016/j.tvjl.2014.11.003. PMID: 25467993.

Chen, V.B., Arendall 3rd, W.B., Headd, J.J., Keedy, D.A., Immormino, R.M., Kapral, G.J., et al., 2010. MolProbity: all-atom structure validation for macromolecular crystallography. Acta Crystallogr. D Biol. Crystallogr. 66 (Pt 1), 12–21. http://dx.doi.org/10.1107/S0907444909042073. PMID: 20057044.

Chen, H.C., Kuo, T.Y., Yang, Y.C., Wu, C.C., Lai, S.S., 2013. Highly permissive subclone of the porcine kidney cell line for porcine circovirus type 2 production. J. Virol. Methods 187 (2), 380–383. http://dx.doi.org/10.1016/j.jviromet.2012.11.013. PMID: 23219808.

Cheung, A.K., 2003. Transcriptional analysis of porcine circovirus type 2. Virology 305 (1), 168–180 PMID: 12504550.

Cruz, T.F., Araujo Jr., J.P., 2014. Cultivation of PCV2 in swine testicle cells using the shell vial technique and monitoring of viral replication by qPCR and RT-qPCR. J. Virol. Methods 196, 82–85. http://dx.doi.org/10.1016/j.jviromet.2013.10.025. PMID: 24183921.

de Boisséson, C., Béven, V., Bigarré, L., Thiéry, R., Rose, N., Eveno, E., et al., 2004. Molecular characterization of Porcine circovirus type 2 isolates from post-weaning multisystemic wasting syndrome-affected and non-affected pigs. J. Gen. Virol. 85 (Pt 2), 293–304. http://dx.doi.org/10.1099/vir.0.19536-0. PMID: 14769887.

DeLano, W.L., 2002. The PyMOL Molecular Graphics System. Available from:. DeLano Scientific, San Carlos, CA, USA. http://www.pymol.org/.

Dolinsky, T.J., Nielsen, J.E., McCammon, J.A., Baker, N.A., 2004. PDB2PQR: an automated pipeline for the setup of Poisson-Boltzmann electrostatics calculations. Nucleic Acids Res. 32, W665–667. http://dx.doi.org/10.1093/nar/gkh381. PMID: 15215472.

Dolinsky, T.J., Czodrowski, P., Li, H., Nielsen, J.E., Jensen, J.H., Klebe, G., et al., 2007. PDB2PQR: expanding and upgrading automated preparation of biomolecular structures for molecular simulations. Nucleic Acids Res. 35, W522–525. http://dx.doi.org/10.1093/nar/gkm276. PMID: 17488841.

Duffy, S., Shackelton, L.A., Holmes, E.C., 2008. Rates of evolutionary change in viruses: patterns and determinants. Nat. Rev. Genet. 9 (4), 267–276. http://dx.doi.org/10.1038/nrg2323. PMID: 18319742.

Dupont, K., Nielsen, E.O., Baekbo, P., Larsen, L.E., 2008. Genomic analysis of PCV2 isolates from Danish archives and a current PMWS case-control study supports a shift in genotypes with time. Vet. Microbiol. 128 (1-2), 56–64. http://dx.doi.org/10.1016/j.vetmic.2007.09.016. PMID: 17996404.

Duran, X., Vilahur, G., Badimon, L., 2009. Exogenous in vivo NO-donor treatment preserves p53 levels and protects vascular cells from apoptosis. Atherosclerosis 205 (1), 101–106. http://dx.doi.org/10.1016/j.atherosclerosis.2008.11.016. PMID: 19124124.

Dvorak, C.M., Puvanendiran, S., Murtaugh, M.P., 2013. Cellular pathogenesis of porcine circovirus type 2 infection. Virus Res. 174 (1-2), 60–68. http://dx.doi.org/10.1016/j.virusres.2013.03.001. PMID: 23499996.

Ellis, J., Hassard, L., Clark, E., Harding, J., Allan, G., Willson, P., et al., 1998. Isolation of circovirus from lesions of pigs with postweaning multisystemic wasting syndrome. Can. Vet. J. 39 (1), 44–51 PMID: 9442952.

Fenaux, M., Opriessnig, T., Halbur, P.G., Elvinger, F., Meng, X.J., 2004. Two amino acid mutations in the capsid protein of type 2 porcine circovirus (PCV2) enhanced PCV2 replication in vitro and attenuated the virus in vivo. J. Virol. 78 (24), 13440–13446. http://dx.doi.org/10.1128/JVI.78.24.13440-13446.2004. PMID: 15564454.

Firth, C., Charleston, M.A., Duffy, S., Shapiro, B., Holmes, E.C., 2009. Insights into the evolutionary history of an emerging livestock pathogen: porcine circovirus 2. J. Virol. 83 (24), 12813–12821. http://dx.doi.org/10.1128/JVI.01719-09. PMID: 19812157.

Fort, M., Sibila, M., Nofrarías, M., Pérez-Martín, E., Olvera, A., Mateu, E., et al., 2010. Porcine circovirus type 2 (PCV2) Cap and Rep proteins are involved in the development of cell-mediated immunity upon PCV2 infection. Vet. Immunol. Immunopathol. 137 (3-4), 226–234. http://dx.doi.org/10.1016/j.vetimm.2010.05.013. PMID: 20566220.

Franzo, G., Cortey, M., de Castro, A.M., Piovezan, U., Szabo, M.P., Drigo, M., et al., 2015a. Genetic characterisation of Porcine circovirus type 2 (PCV2) strains from feral pigs in the Brazilian Pantanal: an opportunity to reconstruct the history of PCV2 evolution. Vet. Microbiol. 178 (1-2), 158–162. http://dx.doi.org/10.1016/j.vetmic.2015.05.003. PMID: 25975522.

Franzo, G., Cortey, M., Olvera, A., Novosel, D., Castro, A.M., Biagini, P., et al., 2015b. Revisiting the taxonomical classification of Porcine Circovirus type 2 (PCV2): still a real challenge. Virol J. 12 (131). http://dx.doi.org/10.1186/s12985-015-0361-x. PMID: 26311322.

Freshney, R.I., 2000. Characterization. In: Freshney, R.I. (Ed.), Culture of Animal Cells: a Manual of Basic Technique. Wiley-Liss, New York, pp. 229–257.

Gao, M., Skolnick, J., 2012. The distribution of ligand-binding pockets around protein-protein interfaces suggests a general mechanism for pocket formation. Proc. Natl. Acad. Sci. U. S. A. 109 (10), 3784–3789. http://dx.doi.org/10.1073/pnas.1117768109. PMID: 22355140.

Grau-Roma, L., Crisci, E., Sibila, M., López-Soria, S., Nofrarias, M., Cortey, M., et al., 2008. A proposal on porcine circovirus type 2 (PCV2) genotype definition and their relation with postweaning multisystemic wasting syndrome (PMWS) occurrence. Vet. Microbiol. 128 (1-2), 23–35. http://dx.doi.org/10.1016/j.vetmic.2007.09.007. PMID: 17976930.

Guo, L.J., Lu, Y.H., Wei, Y.W., Huang, L.P., Liu, C.M., 2010. Porcine circovirus type 2 (PCV2): genetic variation and newly emerging genotypes in China. Virol. J. 7 (273). http://dx.doi.org/10.1186/1743-422X-7-273. PMID: 20955622.

Guo, L., Lu, Y., Wei, Y., Huang, L., Wu, H., Liu, C., 2011. Porcine circovirus genotype 2a (PCV2a) and genotype 2b (PCV2b) recombinant mutants showed significantly enhanced viral replication and altered antigenicity in vitro. Virology 419 (2), 57–63. http://dx.doi.org/10.1016/j.virol.2011.08.004. PMID: 21890163.

Guo, L., Fu, Y., Wang, Y., Lu, Y., Wei, Y., Tang, Q., et al., 2012. A porcine circovirus type 2 (PCV2) mutant with 234 amino acids in capsid protein showed more virulence in vivo, compared with classical PCV2a/b strain. PLoS One 7 (7), e41463. http://dx.doi.org/10.1371/journal.pone.0041463. PMID: 22829951.

Hall, T.A., 1999. BioEdit: a user-friendly biological sequence alignment editor and analysis program for windows 95/98/NT. Nucleic Acids Symp. Ser. (41), 95–98.

Hamel, A.L., Lin, L.L., Nayar, G.P., 1998. Nucleotide sequence of porcine circovirus associated with postweaning multisystemic wasting syndrome in pigs. J. Virol. 72 (6), 5262–5267 PMID: 9573301.

He, J., Cao, J., Zhou, N., Jin, Y., Wu, J., Zhou, J., 2013. Identification and functional analysis of the novel ORF4 protein encoded by porcine circovirus type 2. J. Virol. 87 (3), 1420–1429. http://dx.doi.org/10.1128/JVI.01443-12. PMID: 23152517.

Huang, B., Schroeder, M., 2006. LIGSITEcsc: predicting ligand binding sites using the connolly surface and degree of conservation. BMC Struct. Biol. 6, 19. http://dx.doi.org/10.1186/1472-6807-6-19. PMID: 16995956.

Huang, L.P., Lu, Y.H., Wei, Y.W., Guo, L.J., Liu, C.M., 2011. Identification of one critical amino acid that determines a conformational neutralizing epitope in the capsid protein of porcine circovirus type 2. BMC Microbiol. 11, 188. http://dx.doi.org/10.1186/1471-2180-11-188. PMID: 21859462.

Humphrey, W., Dalke, A., Schulten, K., 1996. VMD: visual molecular dynamics. J. Mol. Graph. 14 (1), 33–38 27-28. PMID: 8744570.

Karuppannan, A.K., Liu, S., Jia, Q., Selvaraj, M., Kwang, J., 2010. Porcine circovirus type 2 ORF3 protein competes with p53 in binding to Pirh2 and mediates the deregulation of p53 homeostasis. Virology 398 (1), 1–11. http://dx.doi.org/10.1016/j.virol.2009.11.028. PMID: 20004925.

Kearse, M., Moir, R., Wilson, A., Stones-Havas, S., Cheung, M., Sturrock, S., et al., 2012. Geneious basic: an integrated and extendable desktop software platform for the organization and analysis of sequence data. Bioinformatics 28 (12), 1647–1649. http://dx.doi.org/10.1093/bioinformatics/bts199. PMID: 22543367.

Khayat, R., Brunn, N., Speir, J.A., Hardham, J.M., Ankenbauer, R.G., Schneemann, A., et al., 2011. The 2.3-angstrom structure of porcine circovirus 2. J. Virol. 85 (15), 7856–7862. http://dx.doi.org/10.1128/JVI.00737-11. PMID: 21632760.

Ladekjaer-Mikkelsen, A.S., Nielsen, J., Stadejek, T., Storgaard, T., Krakowka, S., Ellis, J., et al., 2002. Reproduction of postweaning multisystemic wasting syndrome (PMWS) in immunostimulated and non-immunostimulated 3-week-old piglets experimentally infected with porcine circovirus type 2 (PCV2). Vet. Microbiol. 89 (2-3), 97–114.

Larionov, A., Krause, A., Miller, W., 2005. A standard curve based method for relative real time PCR data processing. BMC Bioinform. 6 (62). http://dx.doi.org/10.1186/1471-

2105-6-62. PMID: 15780134.
Larkin, M.A., Blackshields, G., Brown, N.P., Chenna, R., McGettigan, P.A., McWilliam, H., et al., 2007. Clustal W and Clustal X version 2.0. Bioinformatics 23 (21), 2947–2948. http://dx.doi.org/10.1093/bioinformatics/btm404. PMID: 17846036.
Larochelle, R., Antaya, M., Morin, M., Magar, R., 1999. Typing of porcine circovirus in clinical specimens by multiplex PCR. J. Virol. Methods 80 (1), 69–75 PMID: 10403678.
Larochelle, R., Magar, R., D'Allaire, S., 2002. Genetic characterization and phylogenetic analysis of porcine circovirus type 2 (PCV2) strains from cases presenting various clinical conditions. Virus Res. 90 (1–2), 101–112 PMID: 12457966.
Lekcharoensuk, P., Morozov, I., Paul, P.S., Thangthumniyom, N., Wajjawalku, W., Meng, X.J., 2004. Epitope mapping of the major capsid protein of type 2 porcine circovirus (PCV2) by using chimeric PCV1 and PCV2. J. Virol. 78 (15), 8135–8145. http://dx.doi.org/10.1128/JVI.78.15.8135-8145.2004. PMID: 15254185.
Lindahl, T., Nyberg, B., 1974. Heat-induced deamination of cytosine residues in deoxyribonucleic acid. Biochemistry 13 (16), 3405–3410 PMID: 4601435.
Liu, J., Thorp, S.C., 2002. Cell surface heparan sulfate and its roles in assisting viral infections. Med. Res. Rev. 22 (1), 1–25 PMID: 11746174.
Liu, J., Chen, I., Kwang, J., 2005. Characterization of a previously unidentified viral protein in porcine circovirus type 2-infected cells and its role in virus-induced apoptosis. J. Virol. 79 (13), 8262–8274. http://dx.doi.org/10.1128/JVI.79.13.8262-8274.2005. PMID: 15956572.
Liu, J., Zhu, Y., Chen, I., Lau, J., He, F., Lau, A., et al., 2007. The ORF3 protein of porcine circovirus type 2 interacts with porcine ubiquitin E3 ligase Pirh2 and facilitates p53 expression in viral infection. J. Virol. 81 (17), 9560–9567. http://dx.doi.org/10.1128/JVI.00681-07. PMID: 17581998.
Liu, J., Huang, L., Wei, Y., Tang, Q., Liu, D., Wang, Y., et al., 2013. Amino acid mutations in the capsid protein produce novel porcine circovirus type 2 neutralizing epitopes. Vet. Microbiol. 165 (3-4), 260–267. http://dx.doi.org/10.1016/j.vetmic.2013.03.013. 30; PMID: 23582511.
Mahé, D., Blanchard, P., Truong, C., Arnauld, C., Le Cann, P., Cariolet, R., et al., 2000. Differential recognition of ORF2 protein from type 1 and type 2 porcine circoviruses and identification of immunorelevant epitopes. J. Gen. Virol. 81 (Pt 7), 1815–1824. http://dx.doi.org/10.1099/0022-1317-81-7-1815. PMID: 10859388.
Meehan, B.M., McNeilly, F., Todd, D., Kennedy, S., Jewhurst, V.A., Ellis, J.A., et al., 1998. Characterization of novel circovirus DNAs associated with wasting syndromes in pigs. J. Gen. Virol. 79 (Pt 9), 2171–2179. http://dx.doi.org/10.1099/0022-1317-79-9-2171. PMID: 9747726.
Meerts, P., Misinzo, G., McNeilly, F., Nauwynck, H.J., 2005. Replication kinetics of different porcine circovirus 2 strains in PK-15 cells, fetal cardiomyocytes and macrophages. Arch. Virol. 150 (3), 427–441. http://dx.doi.org/10.1007/s00705-004-0444-2. PMID: 15578238.
Misinzo, G., Delputte, P.L., Meerts, P., Lefebvre, D.J., Nauwynck, H.J., 2006. Porcine circovirus 2 uses heparan sulfate and chondroitin sulfate B glycosaminoglycans as receptors for its attachment to host cells. J. Virol. 80 (7), 3487–3494. http://dx.doi.org/10.1128/JVI.80.7.3487-3494.2006. PMID: 16537616.
Nawagitgul, P., Morozov, I., Bolin, S.R., Harms, P.A., Sorden, S.D., Paul, P.S., 2000. Open reading frame 2 of porcine circovirus type 2 encodes a major capsid protein. J. Gen. Virol. 81 (Pt 9), 2281–2287. http://dx.doi.org/10.1099/0022-1317-81-9-2281. PMID: 10950986.
Nguyen, V.G., Kim, H.K., Moon, H.J., Park, S.J., Keum, H.O., Rho, S., et al., 2012. Population dynamics and ORF3 gene evolution of porcine circovirus type 2 circulating in Korea. Arch. Virol. 157 (5), 799–810. http://dx.doi.org/10.1007/s00705-012-1234-x. PMID: 22289963.
Opriessnig, T., McKeown, N.E., Zhou, E.M., Meng, X.J., Halbur, P.G., 2006. Genetic and experimental comparison of porcine circovirus type 2 (PCV2) isolates from cases with and without PCV2-associated lesions provides evidence for differences in virulence. J. Gen. Virol. 87 (Pt 10), 2923–2932. http://dx.doi.org/10.1099/vir.0.82099-0. PMID: 16963751.
Ritchie, P.A., Anderson, I.L., Lambert, D.M., 2003. Evidence for specificity of psittacine beak and feather disease viruses among avian hosts. Virology 306 (1), 109–115 PMID: 12620803.
Rostand, K.S., Esko, J.D., 1997. Microbial adherence to and invasion through proteoglycans. Infect. Immun. 65 (1), 1–8 PMID: 8975885.
Saha, D., Huang, L., Bussalleu, E., Lefebvre, D.J., Fort, M., Van Doorsselaere, J., et al., 2012a. Antigenic subtyping and epitopes' competition analysis of porcine circovirus type 2 using monoclonal antibodies. Vet. Microbiol. 157 (1-2), 13–22. http://dx.doi.org/10.1016/j.vetmic.2011.11.030. PMID: 22176764.
Saha, D., Lefebvre, D.J., Ooms, K., Huang, L., Delputte, P.L., Van Doorsselaere, J., et al., 2012b. Single amino acid mutations in the capsid switch the neutralization phenotype of porcine circovirus 2. J. Gen. Virol. 93 (Pt 7), 1548–1555. http://dx.doi.org/10.1099/vir.0.042085-0. PMID: 22492916.
Segalés, J., 2012. Porcine circovirus type 2 (PCV2) infections: clinical signs, pathology and laboratory diagnosis. Virus Res. 164 (1–2), 10–19. http://dx.doi.org/10.1016/j.virusres.2011.10.007. PMID: 22056845.
Segalés, J., Olvera, A., Grau-Roma, L., Charreyre, C., Nauwynck, H., Larsen, L., et al., 2008. PCV-2 genotype definition and nomenclature. Vet. Rec. 162 (26), 867–868 PMID: 18587066.
Segalés, J., Kekarainen, T., Cortey, M., 2013. The natural history of porcine circovirus type 2: from an inoffensive virus to a devastating swine disease? Vet. Microbiol. 165 (1-2), 13–20. http://dx.doi.org/10.1016/j.vetmic.2012.12.033. PMID: 23380460.
Seo, H.W., Park, C., Kang, I., Choi, K., Jeong, J., Park, S.J., et al., 2014. Genetic and antigenic characterization of a newly emerging porcine circovirus type 2b mutant first isolated in cases of vaccine failure in Korea. Arch. Virol. 159 (11), 3107–3111. http://dx.doi.org/10.1007/s00705-014-2164-6. PMID: 25034669.
Ssemadaali, M.A., Ilha, M., Ramamoorthy, S., 2015. Genetic diversity of porcine circovirus type 2 and implications for detection and control. Res. Vet. Sci. 103, 179–186. http://dx.doi.org/10.1016/j.rvsc.2015.10.006. PMID: 26679815.
Tamura, K., Peterson, D., Peterson, N., Stecher, G., Nei, M., Kumar, S., 2011. MEGA5: molecular evolutionary genetics analysis using maximum likelihood, evolutionary distance, and maximum parsimony methods. Mol. Biol. Evol. 28 (10), 2731–2739. http://dx.doi.org/10.1093/molbev/msr121. PMID: 21546353.
Timmusk, S., Wallgren, P., Brunborg, I.M., Wikström, F.H., Allan, G., Meehan, B., et al., 2008. Phylogenetic analysis of porcine circovirus type 2 (PCV2) pre- and post-epizootic postweaning multisystemic wasting syndrome (PMWS). Virus Genes 36 (3), 509–520. http://dx.doi.org/10.1007/s11262-008-0217-1. PMID: 18343985.
Vanderplasschen, A., Bublot, M., Dubuisson, J., Pastoret, P.P., Thiry, E., 1993. Attachment of the gammaherpesvirus bovine herpesvirus 4 is mediated by the interaction of gp8 glycoprotein with heparinlike moieties on the cell surface. Virology 196 (1), 232–240. http://dx.doi.org/10.1006/viro.1993.1471. PMID: 8356795.
Wen, L., Guo, X., Yang, H., 2005. Genotyping of porcine circovirus type 2 from a variety of clinical conditions in China. Vet. Microbiol. 110 (1-2), 141–146. http://dx.doi.org/10.1016/j.vetmic.2005.07.003. PMID: 16105722.
Wiederstein, M., Sippl, M.J., 2007. ProSA-web: interactive web service for the recognition of errors in three-dimensional structures of proteins. Nucleic Acids Res. 35, W407–410. http://dx.doi.org/10.1093/nar/gkm290. PMID: 17517781.
Xiao, C.T., Halbur, P.G., Opriessnig, T., 2012. Complete genome sequence of a novel porcine circovirus type 2b variant present in cases of vaccine failures in the United States. J. Virol. 86 (22), 12469. http://dx.doi.org/10.1128/JVI.02345-12. PMID: 23087125.
Xiao, C.T., Halbur, P.G., Opriessnig, T., 2015. Global molecular genetic analysis of porcine circovirus type 2 (PCV2) sequences confirms the presence of four main PCV2 genotypes and reveals a rapid increase of PCV2d. Gen. Virol. 96 (Pt 7), 1830–1841. http://dx.doi.org/10.1099/vir.0.000100. PMID: 25711965.